Some remarks on the performance of three advanced soil constitutive models in the small strain region

Author: Piotr Kowalczyk, formerly University of Trento (Italy)

Currently Research Fellow at University of Southampton (UK)

Email address: p.kowalczyk@soton.ac.uk

Abstract

This short communication identifies some inconsistencies in the numerical predictions of three advanced soil constitutive models. The chosen constitutive models are subject to simple numerical tests in the small strain range relevant to the cyclic response of soil in seismic, offshore and urban applications. The numerical tests comprise: a cyclic simple shear test in the small strain range, a simple shear test with very small strain unloading-reloading loops, and a test on the dependence of the rate of the shear stiffness degradation with increasing shear strain on changing mean confining stress. The results are briefly discussed and, in some cases, the reasons for the observed inconsistencies and potential improvements in the formulations of the investigated constitutive models are initially drafted.

Keywords: constitutive modelling, small strain behaviour, elastoplasticity, hypoplasticity, shear wave propagation, offshore loading, overshooting

1. Background

Numerous advanced soil constitutive models have been developed for modelling soil behaviour in the small strain region. Examples of such models from various constitutive frameworks could include, for instance: paraelastic model [1], classical elastoplastic model [2], multilaminate model [3], representatives of barodesy [4] or bounding surface plasticity models [5, 6]; and many more as listed recently in [7]. Among many constitutive approaches, the research community and practising engineers often opt for the framework of SANISAND (Simple ANIsotropic SAND) elastoplasticity [8-9] or hypoplasticity [10-11] when modelling soil and soil-structure interaction in boundary value problems, including problems related to cyclic loading in seismic, offshore and urban geotechnical engineering. In fact, numerous studies used the SANISAND model (e.g. [12-18]) or the hypoplastic model (e.g. [18-25]) to simulate various boundary value problems. Those two constitutive approaches constitute also a common basis for further developments in soil constitutive modelling (e.g. [26-28] for SANISAND models; [29-31] for hypoplastic models). In addition to those two constitutive frameworks, other promising developments with available implementations in the multiaxial space can be found in literature when considering analysing boundary value problems, for example the updated Severn-Trent model [32] or the HS-Brick model [33]. Although all these constitutive models were shown to successfully reproduce various aspects of soil small strain and cyclic behaviour, there is constant need for validation studies reporting limitations of advanced soil constitutive models (e.g. [34-37]).

This short communication presents three advanced sand constitutive models, namely, the Dafalias-Manzari sand model [9], the hypoplastic sand model [10, 11] and the Severn-Trent sand model [32] regarding their performance in capturing chosen aspects of the small strain behaviour relevant to shear wave propagation in earthquakes and cyclic loading in offshore and urban applications. To this aim, the response of the constitutive models to simple shear stress path loading is analysed in simple numerical tests. The numerical tests include: cyclic simple shear tests in the small strain range (up to 0.1%), simple shear tests in the small strain range with very small strain unloading-reloading loops (0.001% and 0.0001%) and verification of the ability of the constitutive models to simulate accurately the dependence of the rate of the soil stiffness degradation with increasing shear strain on changing mean confining stress. The computations of the constitutive models are compared with each other and, where available, with experimental data. Some inconsistencies in the computed responses are found and discussed in the context of the current formulations and the potential future improvements in the formulations of the models.

2. Methodology

The description of the formulation of the three advanced soil constitutive models, namely the Dafalias-Manzari (DM) model [9], the hypoplastic (HP) model [10, 11] and the Severn-Trent (ST) model [32], can be found in the given references and is not repeated herein for brevity. The implementations of the constitutive models (DM model and HP model [38], ST model [39]) in a 'umat' (User MATerial) format have been used. Note that the implementation of the ST model [39] has been simplified for the sake of the numerical efficiency and assumes no elastoplastic coupling during cyclic loading.

The constitutive models are used in this study with their original calibrations for replicating Toyoura sand behaviour in laboratory tests, i.e. as per [9] for the DM model, and as per [11][40] for the HP model, whereas the ST model has been calibrated as shown in [32]. This calibration was intended mainly on Hostun sand; however, it was also shown successful when simulating laboratory tests on Toyoura sand [32]. The chosen model parameters are shown in Tables 1, 2 and 3, for the DM model, the HP model and the ST model, respectively.

Note that the author also tested the three constitutive models calibrated for Leighton Buzzard sand, fraction E (as shown in [41]) and the HP model with different calibration for Toyoura sand [42]. These calibrations resulted in the same trends as those reported herein but were omitted in this work for brevity with the original calibrations of the constitutive models being preferred in order to limit the potential uncertainties related to the author-derived calibrations.

The numerical predictions of the constitutive models for a cyclic simple shear test compared with laboratory data on Toyoura sand [43] are shown on Figure 1 proving that the calibrations chosen in this paper are able to simulate with satisfactory accuracy cyclic response of sand in simple shear under intermediate strain levels. In short, it can be observed that all the constitutive models predict compressive volumetric response and, generally, slight increase in stiffness with increasing number of loading cycles, thus in agreement with the laboratory data. Note that the predictions of the DM model with e_0=0.756 result in dilative response, thus the initial void ratio was increased to 0.86 to ensure volumetric compression and to adjust the obtained results to those observed in the experiments.

Table 1 Input parameters for DM sand model as derived in [9].

Parameter [unit]	Description	Value
G_0 [-]	Shear modulus constant in the elastic law	125
υ [-]	Poisson's ratio	0.05
m [-]	Size of yield surface	0.01
e_0 [-]	Void ratio on CSL at p=0	0.934
λ_c [-]	Slope of critical state line	0.019
ξ [-]	Critical state line parameter	0.7
M_c [-]	Slope of critical state line in q:p plane, triaxial compression	1.25
c [-]	Control of shape of yield and bounding surfaces in deviatoric section	0.712
h_0 [-]	Plastic modulus constant	7.05
c_h [-]	Plastic modulus constant	0.968
n_b [-]	Plastic modulus constant	1.1
A_0 [-]	Dilatancy constant	0.704
n_d [-]	Dilatancy constant	3.5
z_{max} [-]	Fabric index constant	4
c_z [-]	Fabric index constant	600

Table 2 Input parameters for the hypoplastic sand model as derived in [40] and [11].

	Parameter [unit]	Description	Value
Basic hypoplasticity [40]	φ_c [°]	Critical friction angle	30
	h_s [MPa]	Granular hardness	2600
	n [-]	Stiffness exponent ruling pressure-sensitivity	0.27
	e_{d0} [-]	Limiting minimum void ratio at p'=0 kPa	0.61
	e_{c0} [-]	Limiting void ratio at p'=0 kPa	0.98
	e_{i0} [-]	Limiting maximum void ratio at p'=0 kPa	1.1
	α [-]	Exponent linking peak stress with critical stress	0.18
	β [-]	Stiffness exponent scaling barotropy factor	1.1
Intergranular strain concept [11]	R [-]	Representation of elastic range size	0.0001
	m_R [-]	Stiffness multiplier of the initial stiffness and after 180° change in strain path	5.0
	m_T [-]	Stiffness multiplier after 90° change in strain path	2.0
	β_R [-]	Control of rate of evolution of intergranular strain	0.5
	χ [-]	Control on interpolation between elastic and hypoplastic response	6.0

Table 3 Input parameters for the Severn-Trent sand model as derived in [32].

Parameter [unit]	Description	Value
v_Δ [-]	Intercept for critical-state line in v-ln p' plane at p'=1Pa	2.176
Δ [-]	Slope of critical-state line in v-ln p' plane	0.03
φ_{cv} [°]	Critical-state angle of friction	32
m [-]	Parameter controlling deviatoric section of yield surface	0.8
k [-]	Link between changes in state parameter and current size of yield surface	3.2
A [-]	Multiplier in flow rule	0.75
k_d [-]	State parameter contribution in flow rule	1.3
B [-]	Parameter controlling hyperbolic stiffness relationship	0.016
α [-]	Exponent controlling hyperbolic stiffness relationship	1.8
R [-]	Size of yield surface with respect to strength surface	0.01

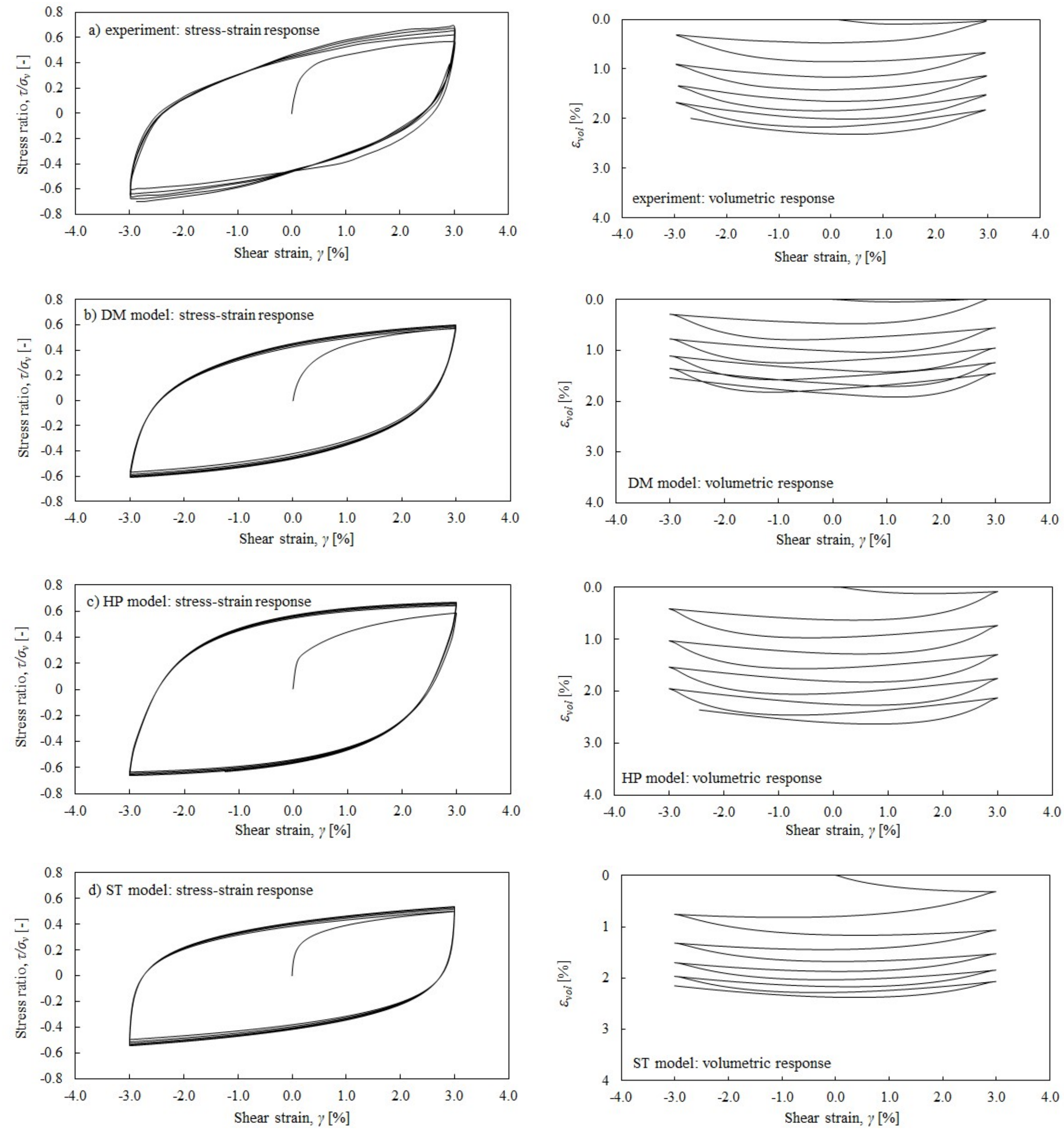

Fig.1 Comparison of numerical simulations with digitalised experimental data from [43] for a cyclic torsional drained simple shear test on Toyoura sand at constant vertical stress of 98kPa and initial isotropic consolidation: a) experimental (e_0=0.756), b) DM model (e_0=0.86), c) HP model (e_0=0.756), d) ST model (e_0=0.756).

The performance of the constitutive models has been inspected in three simple numerical tests carried out in Abaqus [44]. The ability of the constitutive models to deal successfully with the chosen aspects of the small strain behaviour is important when modelling in a reliable manner boundary value problems involving shear wave propagation and cyclic loading in offshore and urban applications.

Note that as the numerical tests are carried out assuming drained response, all the reported stresses in this work should be considered as effective, thus the apostrophe is dropped, and the notation is simplified.

3. Results

Test 1: Cyclic simple shear test in the small strain range (maximum strain of 0.1%)

Figure 2 presents results for a cyclic simple shear test with the same initial conditions as shown for the simple shear tests on Figure 1; however, on this occasion the maximum shear strain is reduced to 0.1% to be representative of the shear strains likely experienced in boundary value problems, for example those dealing with seismic loading conditions.

The results reveal that although the compression is observed in terms of the volumetric response, all the constitutive models predict stiffness reduction with subsequent shearing cycles. It appears that in line with the computed compression, the three constitutive models predict reduction in horizontal stress (Fig. 3) and consequently in mean confining stress (Fig. 4), which apparently may lead to soil stiffness reduction with consecutive load cycles, even though the sample densifies.

Typically, the stress state, including lateral stresses and mean confining stress, is not known in simple shear testing. No experimental data, directly relevant to the comparisons with the carried out numerical test, could be found. However, generally experimental tests suggest that the accumulation of volumetric compressive strain leads to the increase in shear stiffness, as shown for example in [43,45], thus apparently the constitutive models used herein yield less intuitive predictions when the strain level is reduced from 3.0% to 0.1%. Relevant experimental tests could be carried out in the future to explicitly verify these numerical predictions.

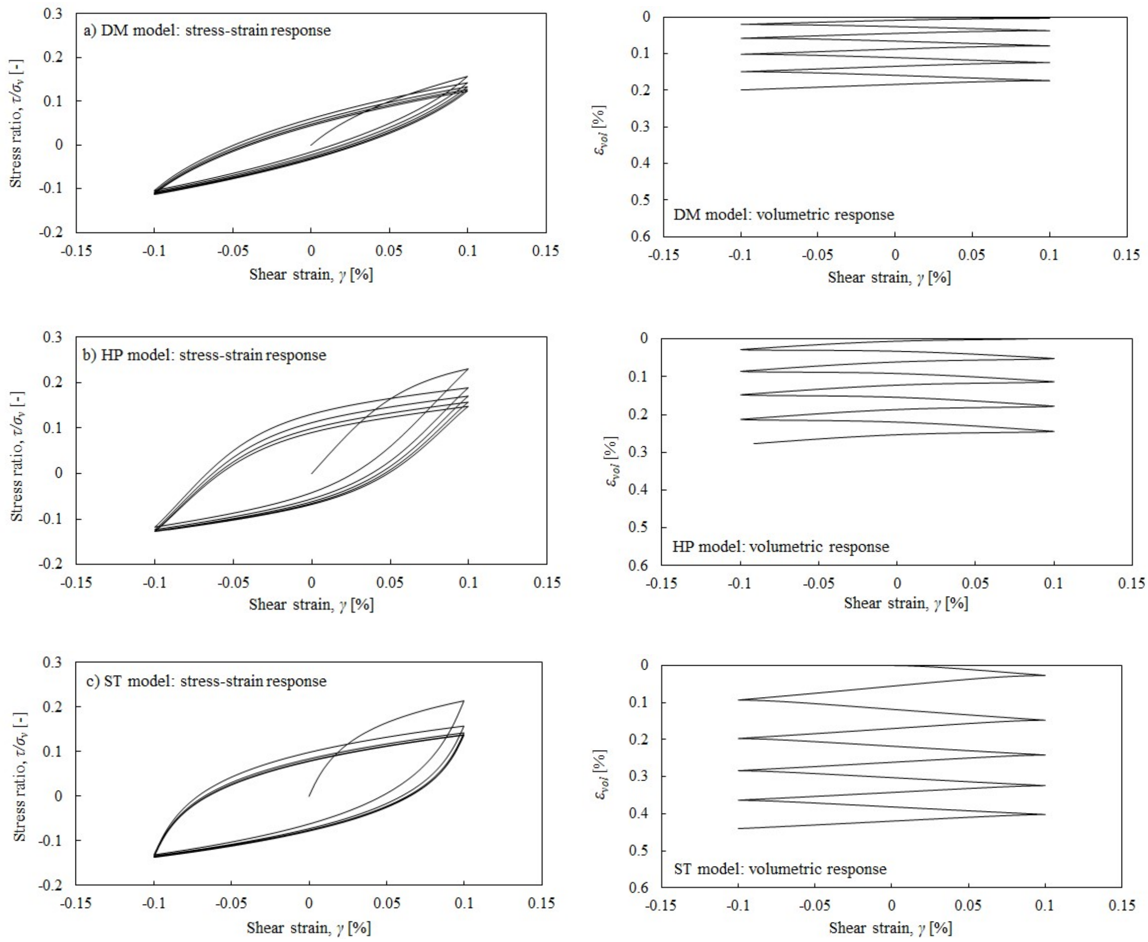

Fig. 2 Comparison of the numerical simulations for cyclic simple shear test in the small strain range: a) DM model, b) HP model, c) ST model.

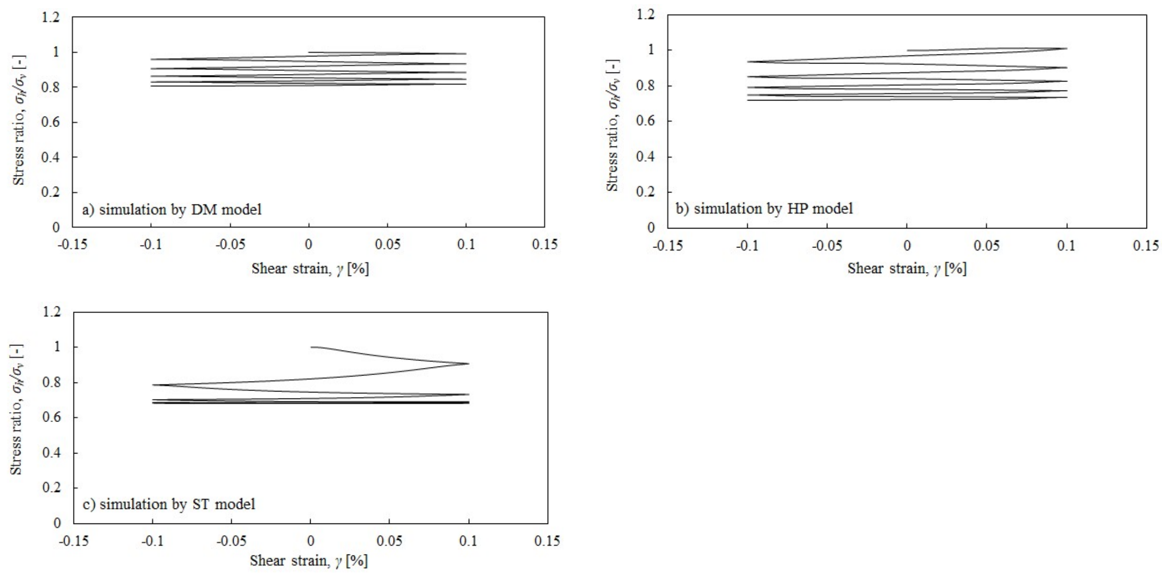

Fig. 3 Changes in the ratio of the horizontal in-plane stress σ_h to the vertical stress σ_v predicted by the three constitutive models: a) DM model, b) HP model, c) ST model.

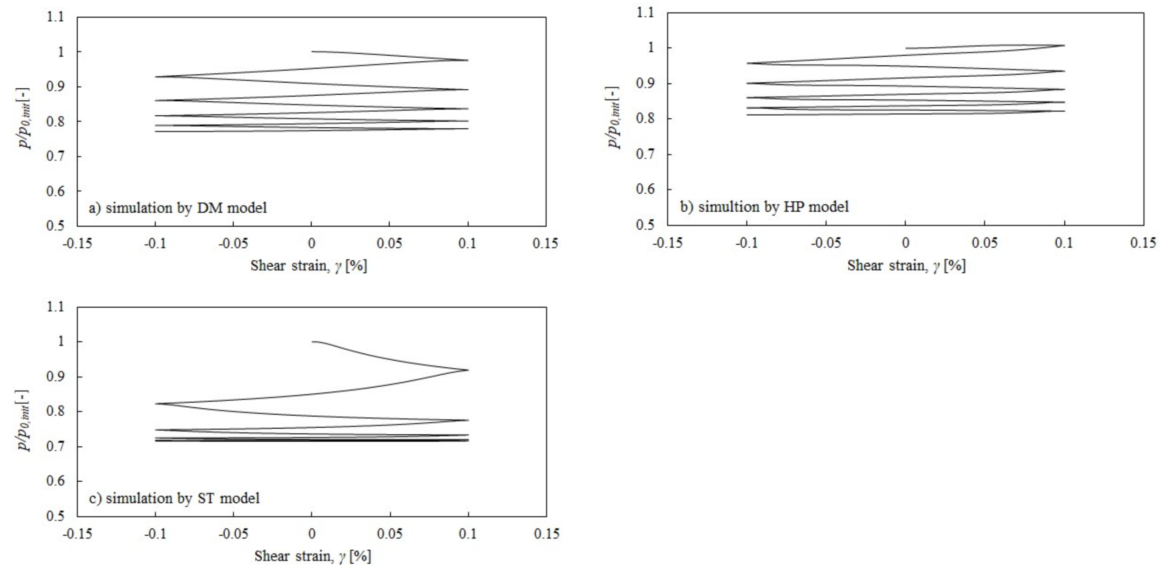

Fig. 4 Changes in mean confining stresses predicted by the three constitutive models: a) DM model, b) HP model, c) ST model.

Test 2: Simple shear test in the small strain range with unloading-reloading loops

A simple shear test is carried out within the small strain range (i.e. maximum shear strain of 0.15%) with very small strain unloading-reloading loops (i.e. 0.001% and 0.01%), to simulate soil response to erratic non-regular shear deformation as likely to happen, for example, under real earthquake loading conditions, due to dynamic disturbance [46], or when modelling in a simplified manner the release and reflections of soil elastic waves in soil dynamic response [47]. The initial conditions for this test are as for Test 1.

The results are shown on Figure 5 and reveal that the ST model strongly overestimates the stiffness on the reloading path when comparing to the predicted monotonic stress path. On the other hand, the HP model slightly overestimates the reloading stiffness and only the DM model is capable of returning to the previous loading path without any noticeable overshooting in the computed stresses. Apparently, the reported trends of overshooting depend on the magnitude of the unloading shear strain. Figure 6 shows the numerical predictions when the unloading-reloading strain cycle is increased to 0.01%. In such case all three models show potentially overshooting response. Note that parametric studies on the vertical stress and density, not shown for brevity in this short communication, confirmed that the general conclusions are independent on those characteristics.

To the best of the author's knowledge, there is no experimental data which could be used as benchmark for the actual direct verification of the speculated herein problem of overshooting of the constitutive models. Some previous experimental works (e.g. [48]) looked at the influence of unloading cycles on the reloading stress path in the intermediate and large strain ranges highlighting that such unloading cycles result in soil densification, thus the increase in soil stiffness and strength on the reloading path could be justified for relatively large unloading-reloading cycles. Nevertheless, excessive overshooting in the reloading path, especially following very small strain unloading (e.g. such as shown by the ST model in Fig. 5c), is rather unexpected and can be deemed as a limitation of the constitutive models.

The problem of overshooting in soil constitutive modelling was acknowledged by some researchers (e.g. [37]). In case of hypoplasticity models, [34] explained that for some reloading paths overshooting effects were encountered. On the other hand, the problem of overshooting in one of the elastoplastic models was critically reviewed in [33, 46]. In this study, the source of the overshooting response in the ST model can be attributed to the constitutive feature of smoothening the stress-strain response between the elastic and plastic stiffnesses. Currently, this constitutive feature depends strongly on the elastic stiffness parameters, and to lesser extent on the plastic stiffness parameters, thus the effect of overshooting will be visible in a stronger manner for a smaller unloading strain (i.e. 0.001%). On the other hand, the case of overshooting response in the DM model may potentially be explained by the well-known characteristic of bounding surface models of an increasing distance to the bounding surface if the unloading strain is large enough to reach the opposite contour of a yield surface. This situation may not happen for a smaller unloading strain (i.e. of 0.001%) when the stress point remains inside the yield surface during the unloading (thus the distance to the bounding surface is not updated) but can happen for a larger unloading strain (i.e. of 0.01%). Finally, it is reminded that there are research works showing constitutive approaches with remediation techniques to overcome overshooting effects (e.g. [1, 49, 50]) thus being potential inspiration for improvements in the tested constitutive models.

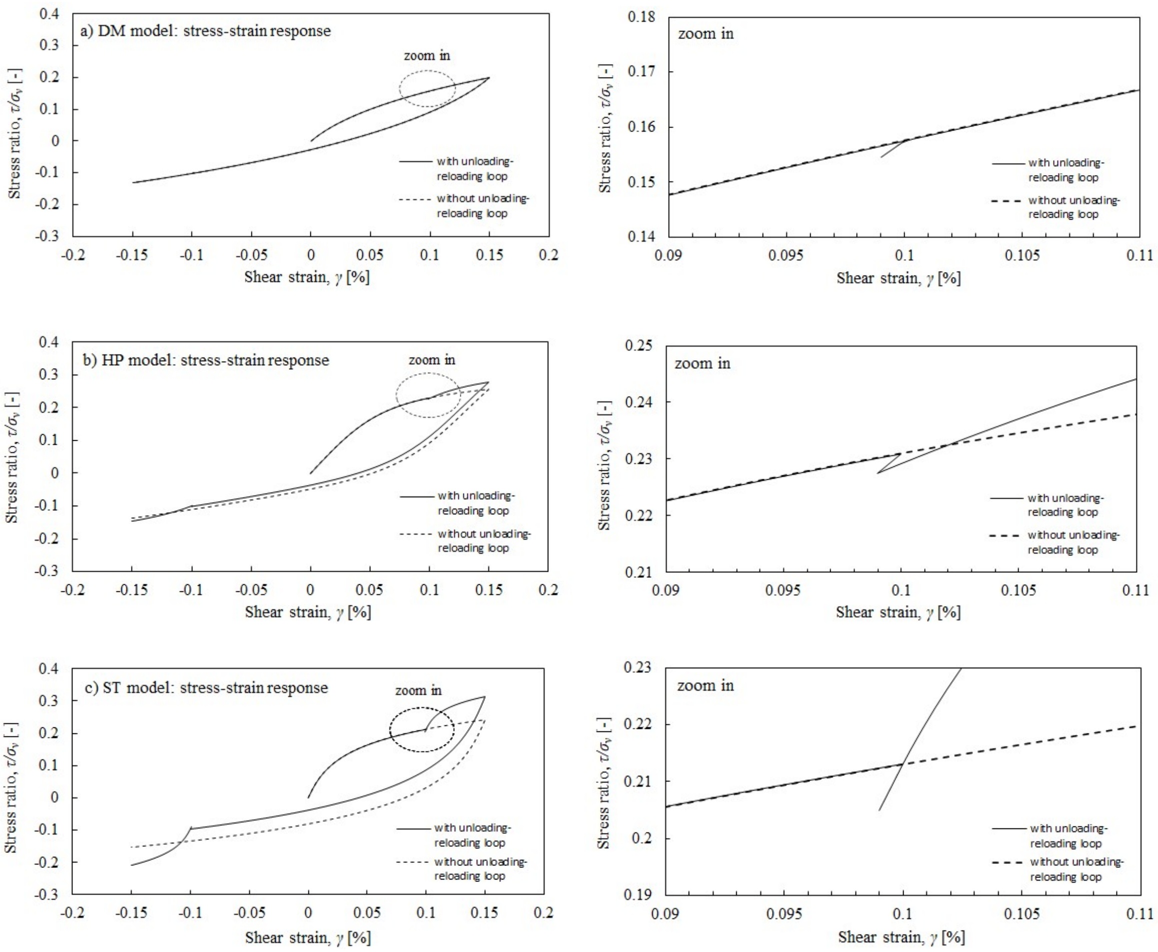

Fig. 5 Comparison of numerical results for simple shear test in small strain range with very small strain unloading-reloading loops (0.001%): a) DM model, b) HP model, c) ST model.

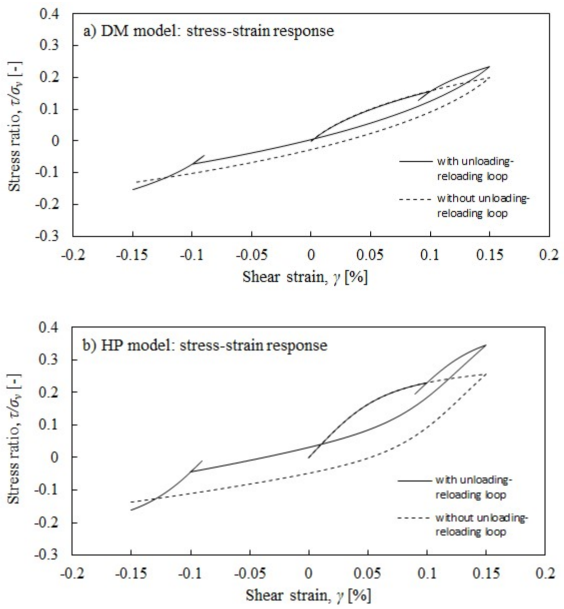

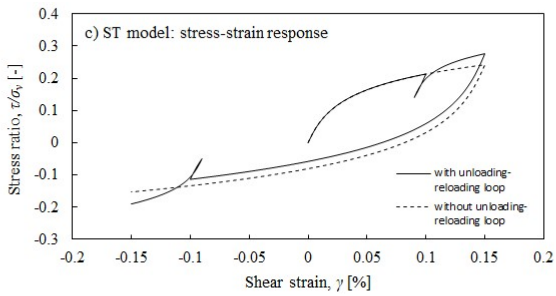

Fig. 6 Comparison of numerical results for simple shear test in small strain range with very small strain unloading-reloading loops (0.01%): a) DM model, b) HP model, c) ST model.

Test 3: Verification of the dependence of the rate of stiffness degradation on changing mean confining stress

Test 3 investigates the ability of the constitutive models to simulate the rate of the soil shear stiffness degradation with increasing strain level and changing mean confining stress, thus applicable also in monotonic loading scenarios. Figure 7a presents the experimental data on Toyoura sand [51] which showed that the rate of the stiffness degradation strongly depends on the mean confining stress, with the fastest rate of stiffness degradation for lower confining stress (20kPa), and the slowest rate of stiffness degradation for higher confining stress (300kPa). Note that [51] evaluated G/G_0 from triaxial tests however the general trends are the same in other laboratory tests (e.g. [52, 53]) thus can be deemed as applicable to simple shear conditions.

The simulations of the shear stiffness degradation with the increasing strains and under a range of mean confining stresses are shown in Figure 7b-7d. The results reveal that the stiffness degradation curve of G/G_0 computed by the HP model (Fig. 7c) remains practically fixed for the full range of the analysed mean confining stresses. Note that this is not the case of the initial stiffness G_0 which is pressure dependent as explained by others (e.g. [54]). The performance of the ST model and the DM model is apparently more accurate in this respect, which in case of the ST model was also shown in [32] before.

The current formulation of the HP model may affect predictions in boundary value problems where modelled soil is subjected to a wide range of mean confining stresses. In order to improve the predictions of the HP model, modifying the model formulation in such a way that chosen parameters of the intergranular strain concept change with changing mean confining stress could be a simple way to improve the model predictions in the future. Some very initial trials were attempted [41] and are currently being further investigated regarding potential improvements in the formulation of the HP model.

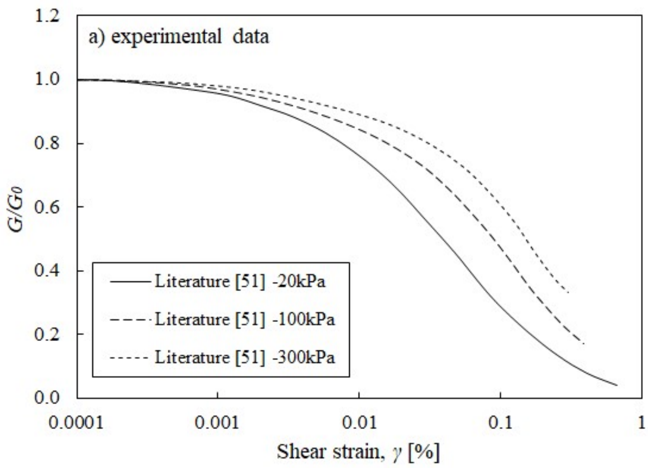

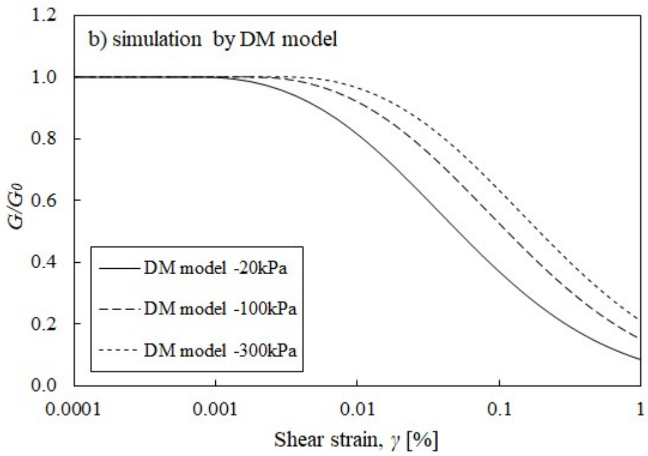

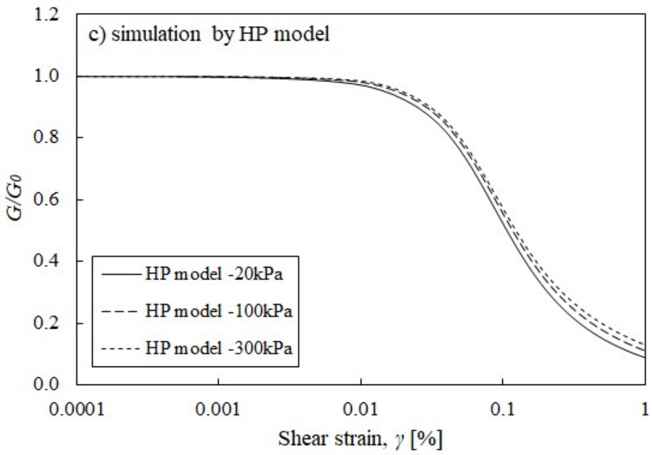

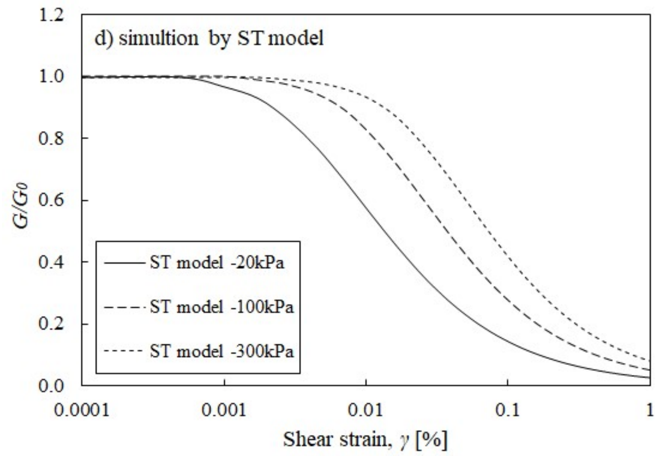

Fig. 7 Stiffness degradation curves G/G_0: a) experimental data [51], b) simulation by the DM model, c) simulation by the HP model, d) simulation by the ST model.

Summary

The performance of three advanced soil constitutive models in chosen aspects of soil small strain behaviour of high relevance to accurate soil modelling in seismic, offshore and urban applications has been shown in this work through simple numerical tests. Some remarks regarding inconsistencies in the predicted responses and limitations of the constitutive models have been highlighted and followed, for chosen cases, by drafting briefly ideas on the reasons of the indicated limitations and the potential improvements in the formulations of the constitutive models for yielding more accurate predictions in the future.

Acknowledgements

This research received funding from the European Union's Horizon 2020 research and innovation programme under the Marie Skłodowska-Curie grant agreement No 721816.

Disclosure Statement

The author has no conflicts of interest to declare.

References

[1] Niemunis, A., Prada-Sarmiento, L.F., Grandas-Tavera, C.E. (2011). Paraelasticity. Acta Geotechnica 6, 67–80.

[2] Gajo, A., Muir Wood, D. (1999). A kinematic hardening constitutive model for sands: the multiaxial formulation. Numerical and Analytical Methods in Geomechanics 23(9), 925-965.

[3] Schädlich, B., Schweiger, H.F. (2012). A multilaminate constitutive model accounting for anisotropic small strain stiffness. International Journal for Numerical and Analytical Methods in Geomechanics 37(10), 1337-1362.

[4] Tafili, M., Medicus, G., Bode, M., Fellin, W. (2022). Comparison of two small-strain concepts: ISA and intergranular strain applied to barodesy. Acta Geotechnica 17, 4333–4358.

[5] Yu, H. S. (1998). CASM: a unified state parameter model for clay and sand. Numerical and Analytical Methods in Geomechanics 22(8), 621-653.

[6] Sternik, K. (2017). Elasto-plastic Constitutive Model for Overconsolidated Clays. International Journal of Civil Engineering 15, 431–440. https://doi.org/10.1007/s40999-017-0193-8

[7] Castellón, J., Ledesma, A. (2022). Small Strains in Soil Constitutive Modelling. Archives of Computational Methods in Engineering 29, 3223–3280. https://doi.org/10.1007/s11831-021-09697-1

[8] Manzari, M. T., Dafalias, Y. F. (1997). A critical state two-surface plasticity model for sands. Géotechnique 47(2), 255-272.

[9] Dafalias, Y., F., Manzari, M. T. (2004). A simple plasticity sand model accounting for fabric change effects. Journal of Engineering Mechanics 130(6), 622-634.

[10] Von Wolffersdorff, P. A. (1996). A hypoplastic relation for granular materials with a predefined limit state surface. Mechanics of Cohesive and Frictional Materials 1(3), 251-271.

[11] Niemunis, A., Herle, I. (1997). Hypoplastic model for cohesionless soils with elastic strain range. Mechanics of Cohesive-Frictional Materials 2, 279-299.

[12] Taiebat, M., Jeremic, B., Dafalias, Y. F., Kaynia, A. M., Cheng, Z. (2010). Propagation of seismic waves through liquified soils. Soil Dynamics and Earthquake Engineering 30(4), 236-257.

[13] Martinelli, M., Burghignoli, A., Callisto, L. (2016). Dynamic response of a plie embedded into a layered soil. Soil Dynamics and Earthquake Engineering 87, 16-28.

[14] Ghofrani, A., Arduino, P. (2018). Prediction of LEAP centrifuge test results using a pressure-dependent bounding surface constitutive model. Soil Dynamics and Earthquake Engineering 113, 758-770.

[15] Kementzetzidis, E., Corciulo, S., Versteijlen, W. G., Pisano, F. (2019). Geotechnical aspects of offshore wind turbine dynamics from 3D non-linear soil-structure simulations. Soil Dynamics and Earthquake Engineering 120, 181-199.

[16] Esfeh, P. K., Kaynia, A. M. (2019). Numerical modelling of liquefaction and its impact on anchor piles for floating offshore structures. Soil Dynamics and Earthquake Engineering 127, 105839.

[17] Eslami, A., Ghorbani, A. (2022). Seismic response of offshore wind turbines supported on Monopiles and Suction Buckets: Numerical modelling and soft computing study. Soil Dynamics and Earthquake Engineering 159, 107284.

[18] Alkhoury, P., Soubra, A.-H., Rey, V., Aït-Ahmed, M. (2022). Dynamic analysis of a monopile-supported offshore wind turbine considering the soil-foundation-structure interaction. Soil Dynamics and Earthquake Engineering 158, 107281.

[19] Hleibieh, J., Wegener, D., Herle, I. (2014). Numerical simulations of a tunnel surrounded by sand under earthquake using a hypoplastic model. Acta Geotechnica 9, 631-640.

[20] Boonyarak, T., Ng, C. W. W. (2014). Effects of construction sequence and cover depth on crossing-tunnel interaction. Canadian Geotechnical Journal 52(7), 851-867.

[21] Mohammadi-Haji, B., Ardakani, A. (2018). Numerical prediction of circular tunnel seismic behaviour using hypoplastic soil constitutive model. International Journal of Geotechnical Engineering 14(4), 428-441, DOI: 10.1080/19386362.2018.1438152

[22] Hleibieh, J., Herle, I. (2019). The performance of a hypoplastic constitutive model in predictions of centrifuge experiments under earthquake conditions. Soil Dynamics and Earthquake Engineering, 122, 310-317.

[23] Yilmaz, S. A., Ercan Tasan, H. (2021). A study on the behaviour of offshore suction bucket foundations under cyclic axial compressive loading. International Journal of Geotechnical Engineering, 16(8), 934-950, DOI: 10.1080/19386362.2021.1995139

[24] Vu, A.-T., Matsumoto, T., Xi, X. & Pham, D.-P. (2022). Behaviours of batter-pile foundations subjected to combination of vertical load and cyclic horizontal loading. International Journal of Geotechnical Engineering, 16(5), 592-605, DOI: 10.1080/19386362.2021.1929696

[25] Kowalczyk, P. (2022). Resonance of a structure with soil elastic waves released in non-linear hysteretic soil upon unloading. Studia Geotechnica et Mechanica 44(4), 253-266.

[26] Pisano, F., Jeremic, B. (2014). Simulating stiffness degradation and damping in soils via a simple visco-elastic-plastic model. Soil Dynamics and Earthquake Engineering 63, 98-109.

[27] Boulanger, R., Ziotopoulou, K. (2015). PM4Sand Version 3: A sand plasticity model for earthquake engineering applications. Technical Report.

[28] Petalas, A., Dafalias, Y. F., Papadimitriou, A. G. (2020). SANISAND-F: Sand constitutive model with evolving fabric anisotropy. International Journal of Solids and Structures 188-189, 12-31.

[29] Wegener, D., Herle, I. (2014). Prediction of permanent soil deformations due to cyclic shearing with a hypoplastic constitutive model. Geotechnik 37(2), 113-122.

[30] Fuentes, W. ,Triantafyllidis, T. (2015). ISA model: a constitutive model for soils with yield surface in the intergranular strain space. International Journal for Numerical and Analytical Methods in Geomechanics 39(11), 1235-1254.

[31] Fuentes, W. ,Wichtmann, T., Gil, M., Lascarro, C. (2020). ISA-Hypoplasticity accounting for cyclic mobility effects for liquefaction analysis. Acta Geotechnica 15(6), 1513-1531.

[32] Gajo, A. (2010). Hyperelastic modelling of small-strain anisotropy of cyclically loaded sand. International Journal for Numerical and Analytical Methods in Geomechanics 34(2), 111-134.

[33] Cudny, M., Truty, A. (2020). Refinement of the Hardening Soil model within small strain range. Acta Geotechnica 15, 2031–2051.

[34] Wichtmann, T., Fuentes, W., Triantafyllidis, T. (2019). Inspection of three sophisticated constitutive models based on monotonic and cyclic tests on fine sand: Hypoplasticity vs. Sanisand vs. ISA. Soil Dynamics and Earthquake Engineering 124, 172-183.

[35] Schranz, F., Fellin, W., Kolymbas, D. (2019). Comparative performance of some constitutive models in stress rotation. Open Geomechanics, article no. 4, 11p. https://doi.org/10.5802/ogeo.3

[36] Jostad, H. P., Misund Dahl, B., Page, A., Sivasithamparam, N., Sturm, H. (2020).

Evaluation of soil models for improved design of offshore wind turbine foundations in dense sand. Géotechnique 70(8), 682-699.

[37] Duque, J., Yang, M., Fuentes, W., Mašín, D., Taiebat, M. (2021). Characteristic limitations of advanced plasticity and hypoplasticity models for cyclic loading of sands. Acta Geotechnica 17, 2235-2257.

[38] Gudehus, G., Amorosi, A., Gens, A., Herle, I., Kolymbas, D., Mašín, D., Muir Wood, D., Nova, R., Niemunis, A., Pastor, M., Tamagnini, C., Viggiani, G. (2008). The soilmodels.info project. International Journal of Numerical and Analytical Methods in Geomechanics 32(12), 1571-1572.

[39] Gajo, A. (2017). Fortran subroutine in a format of User defined MATerial (*UMAT*) of implementation of the Severn-Trent sand model.

[40] Herle, I., Gudehus, G. (1999). Determination of parameters of a hypoplastic constitutive model from properties of grain assemblies. Mechanics of Cohesive and Frictional Materials 4(5), 461-486.

[41] Kowalczyk, P. (2020). Validation and application of advanced soil constitutive models in numerical modelling of soil and soil-structure interaction under seismic loading. PhD Thesis. University of Trento. http://hdl.handle.net/11572/275675

[42] Ng, C. W. W., Boonyarak, T., Mašín, D. (2013). Three-dimensional centrifuge and numerical modelling of the interaction between perpendicularly crossing tunnels. Canadian Geotechnical Journal 50(9), 935-946.

[43] Shahnazari, H., Towhata, I. (2002). Torsion shear tests on cyclic stress-dilatancy relationship of sand. Soils and Foundations 42(1), 105-119.

[44] Dassault Systèmes (2019). Abaqus Standard software package.

[45] Nikitas, G., Arany, L., Aingaran, S., Vimalan, J., Bhattacharya, S. (2017). Predicting long term preformance of offshore wind turbines using cyclic simple shear apparatus. Soil Dynamics and Earthquake Engineering 92, 678-683.

[46] Niemunis, A., Cudny, M. (2018). Discussion on: Dynamic soil-structure interaction: a three-dimensional numerical approach and its application to the Lotung case study. Poor performance of the HSS model. Computers and Geotechnics 98, 243–245.

[47] Kowalczyk, P., Gajo, A. (2022). Introductory consideration supporting the idea of the release of unloading elastic waves in the steady state response of hysteretic soil. Preprint available on: https://doi.org/10.31224/2586

[48] Wichtmann, T., Triantafyllidis, T. (2016). An experimental data base for the development, calibration and verification of constitutive models for sand with focus to cyclic loading. Part II: tests with strain cycles and combined loading. Acta Geotechnica, 11(4), 763-774.

[49] E-Kan, M., Taiebat, H. A. (2014). On implementation of bounding surface plasticity models with no overshooting effect in solving boundary value problems. Computers and Geotechnics 55, 103-116.

[50] Ghorbani, J., Chen, L., Kodikara, J., Carter, J., McCartney, J. (2023). Memory repositioning in soil plasticity models used in contact problems. Computational Mechanics 71, 385–408.

[51] Kokusho, T. (1980). Cyclic triaxial test of dynamic soil properties for wide strain range. Soils and Foundations 20(2), 45-60.

[52] Wichtmann, T., Triantafyllidis, Th. (2004). Influence of a cyclic and dynamic loading history on dynamic properties of dry sand, part I: cyclic and dynamic torsional prestraining. Soil Dynamics and Earthquake Engineering 24(2), 127-147.

[53] Wichtmann, T., Triantafyllidis, Th. (2014). Stiffness and damping of clean quartz sand with various grain size distribution curves. Journal of Geotechnical and Geoenvironmental Engineering 140(3).

[54] Mašín, D. (2018). Modelling of soil behaviour with hypoplasticity. Another approach to soil constitutive modelling. Springer.